

TENSILE TEST MODELS FOR LOW-CARBON MICROALLOYED STEELS WITH HIGH NIOBIUM CONTENTS

Marcos Pérez-Bahillo, Nenad Gubelj, David A. Porter, Beatriz López, Jožef Predan, Antonio Martín-Meizoso

Original scientific paper

In the present investigation, the effect of both: rolling parameters (2 reduction rates and 3 cooling rates) and chemical elements such as: C, Mn, Nb, Ti, Mo, Ni, Cr, Cu and B, has been studied in relation to strength properties in low-carbon microalloyed steels with high niobium contents (up to 0,12 wt. % Nb). For this purpose, an experimental set-up was designed based on an intelligent design of experiments (DoE), resulting in 26 casts (laboratory casts). A combination of metallography, Electron Back-Scattered Diffraction (EBSD) and tensile tests have been performed to study how processing parameters and chemical composition affect the strength. The results, where the proof stress, tensile strength, uniform and fracture elongations are the response variables, have been analysed statistically by means of multiple linear regression technique, leading to response equations. From the results, it was found that the effectiveness of niobium increasing the strength is reduced as carbon content increases.

Key words: microalloyed steels, mechanical properties, niobium

Modeli za ispitivanje rastezne čvrstoće nisko-ugličnih mikrolegiranih čelika s visokim sadržajem niobija

Izvorni znanstveni članak

U ovom se istraživanju proučavao utjecaj parametara valjanja (2 redukcijske brzine i 3 brzine hlađenja) i kemijskih elemenata kao što su: C, Mn, Nb, Ti, Mo, Ni, Cr, Cu i B na svojstva čvrstoće niskougljičnih mikrolegiranih čelika s visokim sadržajem niobija (do 0,12 wt. % Nb). U tu je svrhu konstruiran pokusni uređaj zasnovan na inteligentnom dizajnu eksperimenata (DoE), rezultirajući s 26 odljevaka (laboratorijskih odljevaka). Kombinacijom metalografije, Electron Back-Scattered Diffraction (EBSD) i vlačnih ispitivanja proučavalo se kako obradni parametri i kemijski sastav djeluju na čvrstoću. Kada je ispitivanje rezultiralo naprezanjem, rasteznom čvrstoćom, jednoličnom deformacijom ili deformacijom zbog loma, rezultati su statistički analizirani tehnikom višestrukelinearne regresije, koja je dovela do odgovarajućih jednadžbi. Ustanovilo se da se učinak niobija na povećanje čvrstoće smanjuje kako se povećava sadržaj ugljika.

Ključne riječi: mikrolegirani čelici, mehanička svojstva, niobij

1

Introduction

Strength and toughness are two most important mechanical properties for the design of steel structures, pressure vessels, pipelines or other similar components [1]. Thermo-mechanical rolling is used to maximise grain refinement and thus achieve both higher strength and toughness [2]. A fine grain microstructure is an optimum method for improving strength since unlike most other strengthening mechanisms, the improvement in strength is also accompanied by an improvement in toughness. The use of niobium in low-carbon bainitic steels is advantageous because when the amount of solute niobium is increased, retardation of austenite recrystallization is observed at significant higher temperatures, and also because of its ability to promote the formation of bainite [3, 4]. It is well known that the reduction of carbon contents improves weldability of steels.

2

Intelligent design of experiments

To study the effect of C, Mn, Nb, Ti, Mo, Ni, Cr, Cu and B, a statistical approach is used, by means of an intelligent design of experiments using a three-stage approach:

- ☑ In stage 1, a half fractional factorial design is used to examine five factors at two levels using sixteen casts, the factors being Mn, Ni, Cu, Mo and Cr; 16 casts in total.
- ☑ Stage 2, is a full factorial design, with combinations of low and high levels of C and Nb.
- ☑ Stage 3 investigates the influence of B and Ti since only B in solid solution is effective for the phase transformation.

The levels for each element are shown in Tab. 1.

Table 1 Intelligent design of experiments, laboratory casts

Stage	Level	C	Nb	Ti	B	Mn	Ni	Mo	Cu	Cr
1	Low					1,5	0	0	0	0
	Base	0,04	0,10	0,015	0					
	High					2,1	0,5	0,3	0,5	0,5
2	Low	0,01	0,04							
	Base			0,015	0	1,8	0,25	0,15	0,25	0,25
	High	0,07	0,07							
3	Low			0,008	0,000					
	Base					1,8	0,25	0,15	0,25	0,25
	High			0,025	0,002					

In total, 26 casts: 24 casts with the aim composition from the experimental design, plus 2 failed casts (because of high carbon level: 0,09 wt. %) have been made. From each cast, one 12 mm thickness plate has been rolled under six conditions. These conditions have reduction ratios below the no recrystallization temperature (θ_{nr}) of 2 and 4, with a finish rolling temperature of 850 °C and cooling rates between 850 °C and 550 °C of 0,5 °C/s (Air Cooling, AC), 10 °C/s followed by air cooling (ACcelerated Cooling + Air Cooling, ACC + AC), and 10 °C/s followed by slow cooling (ACcelerated Cooling + Coiling simulation, ACC + CT) as sketched in Fig. 1. All these plates have been supplied by OCAS ArcelorMittal R&D (Belgium).

Tab. 2 summarizes the six rolling conditions. These conditions are selected to simulate the slow cooling conditions in heavy plate mills without accelerated cooling, faster cooling in heavy mills with accelerated cooling, and in hot strip mills with coiling after rolling.

Four industrial casts were used for the verification/validation of the models obtained with the laboratory casts. These industrial casts were delivered by Ruukki (Finland), Corus (United Kingdom) and Salzgitter (Germany).

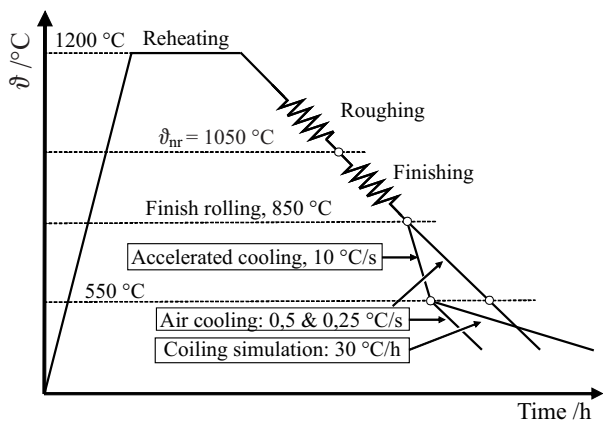


Figure 1 Schematic illustration of the thermomechanical rolling schedule of laboratory casts

Table 2 Rolling schedules

Rolling schedules	Cooling conditions		
	AC	ACC + AC	ACC + CT
RR = 2	C	E	G
RR = 4	D	F	H

Table 3 Analysis (wt. %) of the industrially cast materials

Cast	C	Mn	N	Ti	Nb	V	Ni	Mo	Cu	Cr	Ti/N
81351	0,042	1,97	0,0084	0,015	0,10	0,013	0,21	0,005	0,21	0,98	1,79
02098	0,079	1,66	0,0050	0,003	0,04	0,079	0,06	0,004	0,06	0,04	0,58
16685	0,047	1,73	0,0082	0,018	0,10	0,009	0,04	0,069	0,04	0,27	2,20
81913	0,05	1,58	0,0059	0,016	0,10	0,007	0,16	0,005	0,25	0,26	2,71

3 Experimental methods

3.1 EBSD Technique

The present work deals with different types of microstructures: ferrite, bainite and mixture of the former ones. In most conventional metallographic images, such as optical micrographs, grain boundaries can be distinguished by applying an etchant which attacks grain boundaries preferentially. However, sometimes the low angle misorientations, characteristic of bainite, are not detected. Therefore, the characterization of different types of microstructures by means of conventional metallographic techniques is sometimes hard to carry out. On the other hand, Electron Back-Scattered Diffraction technique (EBSD) is a useful tool to obtain detailed microstructural information, mainly at the scale of bainitic microstructures.

The samples for EBSD observations were prepared from rolling schedules samples, taking into account the rolling direction. All the scans were carried out on a Philips XL30cp Scanning Electron Microscope (SEM) at the quarter plate thickness position. The step size was 0,4 μm and scan size was 160 × 100 μm. TSL OIM Analysis 4.6 software was used to analyse the data.

3.2 Tensile tests

Round tensile test specimens, with 25 mm gauge length and 5 mm cross section diameter, were machined according to standard DIN 10125. Testing was performed by Faculty of Mechanical Engineering, University of Maribor (Slovenia), with an INSTRON 1255 servo hydraulic testing machine supported by Control Panel 8500+. An optical deformation and strain measurement system ARAMIS [18]

was used to determine the stress-strain curves. Duplicate specimens were taken from most plate conditions. From tensile tests, 0,2 % proof stress, tensile strength, uniform and fracture elongations were calculated.

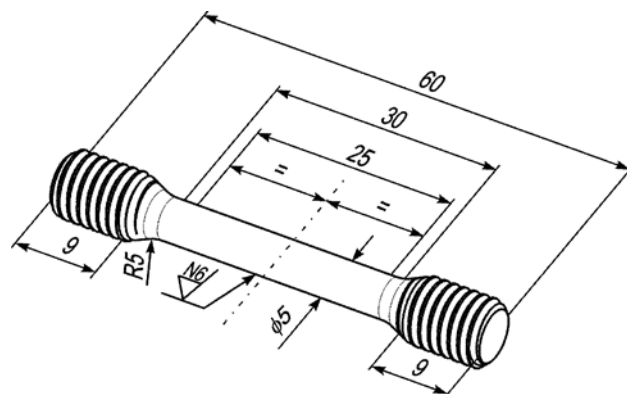


Figure 2 Round tensile specimen used in investigation

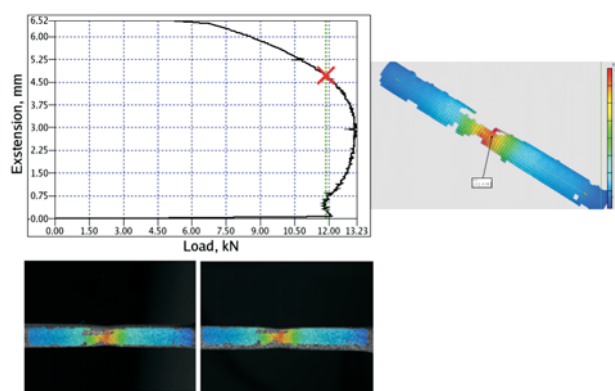


Figure 3 Tensile testing by using 3D optical extensometer

4 Statistical analysis

4.1 Introduction

Multiple linear regression technique was used to obtain response equations from the response variables: proof stress, tensile strength, uniform and fracture elongations. *Essential Regression and Experimental Design of Chemist and Engineers Software*® was employed for this purpose. The sample was formed by the aforementioned 26 casts (laboratory casts) whose results can be found in detail elsewhere [5].

4.2 Response Variables

Concerning response regressors, those parameters or variables considered in the three intelligent designs were taken into account: Chemical elements (C, Nb, Ti, Mn, B, Cr, Cu, Ni and Mo) and rolling parameters: rolling reduction (RR) and cooling rates (where $CR_{800-550\text{ °C}}$ and $CR_{550-20\text{ °C}}$ denote CR_1 and CR_2 , respectively). A transformation of variables takes place concerning the cooling rates (CR_1 , CR_2). Note that the cooling rates are basically between 0,5 – 10 °C/s and 0,25 – 0,008 °C/s for CR_1 and CR_2 , respectively. The cooling rates variables differ by orders of magnitude, being such orders of magnitude which make the difference. Therefore the cooling rates are introduced as the decimal logarithms, $\log_{10}CR_1$ and $\log_{10}CR_2$. For the sake of brevity,

such terms will be spelt as $\lg CR_1$ and $\lg CR_2$ from now on.

Furthermore, based on metallurgical reasons, interaction terms such as; $\lg CR_1 \times$ composition terms, $RR \times \lg CR_1$, $Nb \times \lg CR_2$, $RR \times Nb$, $C \times Nb$ and $Ti \times B$, have been explored in the multiple regressions. The physical meaning of these terms can be explained as follows: In the first place, $\lg CR_1 \times$ composition terms mean the correction that needs to be applied to the chemical elements for the fastest cooling rates (CR_1 , accelerated cooling). As instance, there are elements, such as Mn, B, which present remarkable effects on hardenability (promoting the appearance of bainite), and therefore on strength for air cooling samples. However when accelerated cooling is applied, such effects are weakened, simply because a high proportion of bainite is formed, almost irrespective of Mn or B additions.

In a previous work [6], the microstructure which shows this sort of steels was properly described. From this work, it was found that the effect of accelerated cooling on microstructure depends strongly on the applied rolling reduction. For low reductions ($ACC + RR = 2$), bainite microstructures (almost 100 %) were found, in contrast with those for higher reductions ($ACC + RR = 4$), where a finer microstructure, composed by a mixture of ferrite and bainite, is found. As will be demonstrated later on, the type of microstructure (ferrite, bainite) plays an important role on mechanical properties. For these reasons, the interaction term $RR \times \lg CR_1$ has been included.

The interaction terms $Nb \times \lg CR_2$ and $RR \times Nb$ explain how the effect of Nb can be increased by reducing both CR_2 and rolling reduction; lower cooling rate CR_2 (coiling simulation) allows more time for NbC precipitation, whilst decreasing the rolling reduction below ϑ_{nr} (finishing stage), more Nb is retained in solution in the austenite, prior to phase transformation (γ/α), which can increase strength by increasing the hardenability or precipitation.

Finally concerning $C \times Nb$ and $Ti \times B$, these terms have been considered to study the interaction effects of these two pairs of elements. On the one hand, high additions of Nb (up to 0,12 wt. %) can be more effective with low C levels than with higher contents, when considering the solubility and precipitation of NbC. And on the other, it is well established that only B in solid solution is effective for the phase transformation. Therefore the formation of BN is avoided by means of selected titanium additions, where Ti/N above the stoichiometric ratio ($Ti/N > 3,42$) is expected to be more effective than that below the stoichiometric ratio ($Ti/N < 3,42$).

4.3

Coefficients of multiple determination

In order to figure out whether a model actually describes the data adequately or how good is the "fit" of the predicted data compared to the "real data", the most common coefficient used is the coefficient of determination, R^2 . An R^2 of 1,0 indicates that the regression line perfectly fits the data. However a R^2 value close to unity does not necessarily guarantee a good model; each additional variable added to the model increases R^2 . Thus, R^2 can be made larger simply by adding more predictor variables to the model.

There is another coefficient of determination which bears in mind the degrees of freedom in the model: adjusted coefficient of determination, R^2_{adj} . This adjusted R^2 does not automatically increase when new predictor variables are

added to the model, in fact, the R^2_{adj} may actually decrease. This gives an idea of how much or how little added value is obtained from a bigger model. Finally, another important parameter in the data analysis is the concept of significance, denoted as α . In statistics, a coefficient is significant if it is unlikely to occur by chance; the smaller its significance parameter, the safer the coefficient is. Significance levels of 0,10 and 0,05 are commonly used to determine whether a coefficient is significant or not. In this work, a significance level of $\alpha = 0,1$ has been adopted.

4.4

Response equations

For each parameter, two equations are fitted:

"Autofit": Only those variables with significance $\alpha < 0,1$ are considered and

" R^2_{adj} max": where all possible models are considered and the one with the largest adjusted determination (maximum R^2_{adj}) coefficient is retained.

The first option (Autofit) is the safest statistical approach. The second one is trying to detect some more effects, but the coefficients are not so sure ($\alpha > 0,1$).

5

Results

5.1

Microstructure

As described in detail elsewhere [6], typical microstructures observed for this type of steels, low-carbon microalloyed steels with high niobium contents, can be observed in Fig. 4, by means of Inverse Pole Figures (IPF) and Image Quality maps. The Image Quality map is a map formed by mapping image quality parameter (IQ) obtained from each point in an EBSD scan onto a gray scale. The IQ parameter describes the quality of an electron backscatter diffraction pattern. Any distortions to the crystal lattice, such as grain boundaries (mainly) and high dislocation density within the diffraction volume, produce lower quality (more diffuse) diffraction patterns. Because of the high dislocation density characteristic of bainite, in contrast with ferrite, bainite shows a poorer diffraction pattern which is translated into darker areas.

The air cooling samples (AC) mostly show polygonal ferrite microstructures as shown in Fig. 4a. However, some air cooling samples (AC) show acicular morphologies (bainite), instead of polygonal ferrite, when either boron or high contents of Mn (2,1 %) together with allowing elements such as Ni, Cr and mainly Mo are added. As the accelerated cooling is applied, the type of microstructure changes significantly, polygonal ferrite is replaced by a mixture of lower transformation microstructures, bainite. As said before, the effect of accelerated cooling on grain sizes and microstructure depends strongly on the applied rolling reduction.

For low rolling reductions ($ACC + RR = 2$), bainitic microstructures are found, with a remarkable presence of coarse bainitic packets, see Fig. 4c. Conversely, in the case of higher reduction ($ACC + RR = 4$), a finer microstructure, in comparison with those of air cooling conditions, is achieved, showing a mixture of ferrite and bainite, see Fig. 4b. In essence, the observed microstructures can be classified as follows: ferrite, mixture (ferrite plus bainite) and bainite.

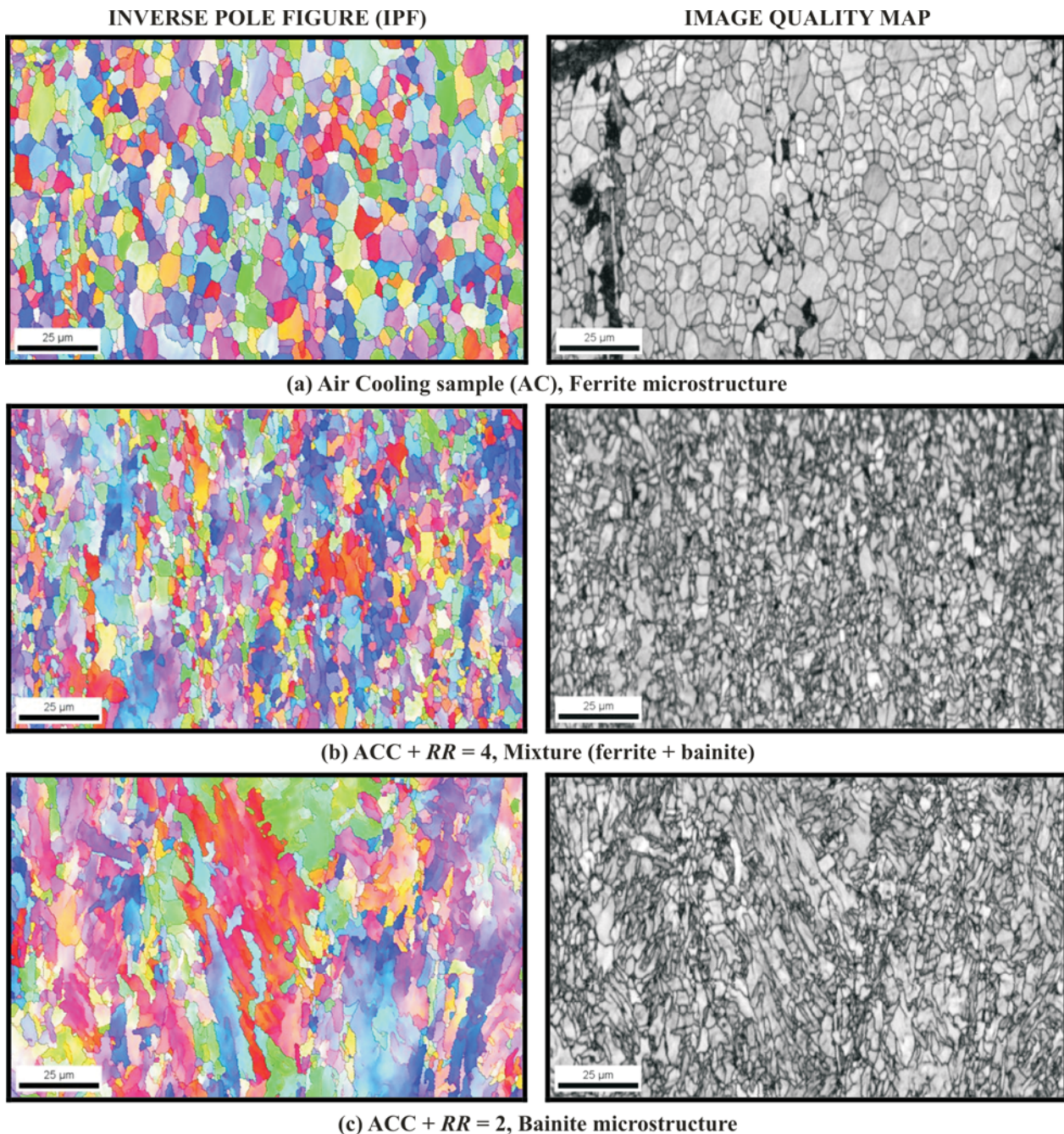


Figure 4 Inverse Pole Figures (IPF) and Image Quality Maps of ferrite, mixture (ferrite plus bainite) and bainite microstructures. 0,025 wt. % C, 1,8 wt. % Mn, 0,05 wt. % Nb, 0,24 wt. % Ni, 0,17 wt. % Mo, 0,27 wt. % Cu and 0,25 wt. % Cr cast.

5.2 Mechanical properties

In order to evaluate the effect of both the rolling parameters (rolling reduction and cooling rates) and type of microstructure on mechanical properties, strength and elongation, data from the 26 laboratory casts have been collected as a function of the aforementioned variables in Tab. 4 and Fig. 5. From these figures, the effect of the type of microstructure on mechanical properties is remarkable. The mean proof stress values are 500, 600 and 650 MPa for ferrite, mixture and bainite, respectively. These latter results are in accordance with the reported ones, where up to a yield strength of about 550 MPa typically relies on ferrite plus pearlite microstructures, while higher strength steels need to have bainitic constituents and steel with about 700 MPa yield strength is typically 100 % bainitic [7]. By applying accelerated cooling, about 100 MPa higher both proof stress

and tensile strength are obtained. This can be explained by the microstructure, which exhibits a more bainitic microstructure rather than ferritic one observed in the air cooling samples.

Unfortunately, the change in strength adversely affects elongation properties; see Fig. 6a, where the change on (uniform) elongation properties follows the strengthening vector. Again, the microstructure plays an important role, see Fig. 5b and Fig. 6b. Both the uniform and fracture elongation values (averages) are reduced from 12,5 and 21,6 % for ferrite, to 8,3 and 17,6 % for mixture (ferrite plus bainite) and to 6,7 and 14,9 % for bainite.

Eventually, it is worth to comment that rolling reduction (*RR*) does not play any role, at first sight, on mechanical properties, see Fig. 5. This point is properly discussed later on.

Table 4 Attainable mechanical properties, as a function of microstructure and processing conditions, for low-carbon microalloyed steels. Mean values and standard deviations.

Mechanical Properties	Proof Stress (MPa)	Tensile Strength (MPa)	Uniform elongation (%)	Elongation of fracture (%)
AC	520 ± 70	650 ± 110	11.2 ± 3.0	19.8 ± 3.9
ACC + AC	610 ± 50	750 ± 70	7.6 ± 2.1	16.5 ± 3.1
ACC+ CT	650 ± 60	760 ± 70	7.7 ± 1.8	16.5 ± 3.5
RR = 2	590 ± 80	720 ± 90	8.6 ± 2.7	17.5 ± 4.1
RR = 4	600 ± 80	720 ± 100	9.1 ± 3.1	17.8 ± 3.5
FERRITE	500 ± 50	610 ± 80	12.5 ± 2.1	21.6 ± 3.1
MIXTURE	600 ± 50	720 ± 60	8.3 ± 1.6	17.6 ± 2.8
BAINITE	650 ± 50	790 ± 60	6.7 ± 1.5	14.9 ± 2.4

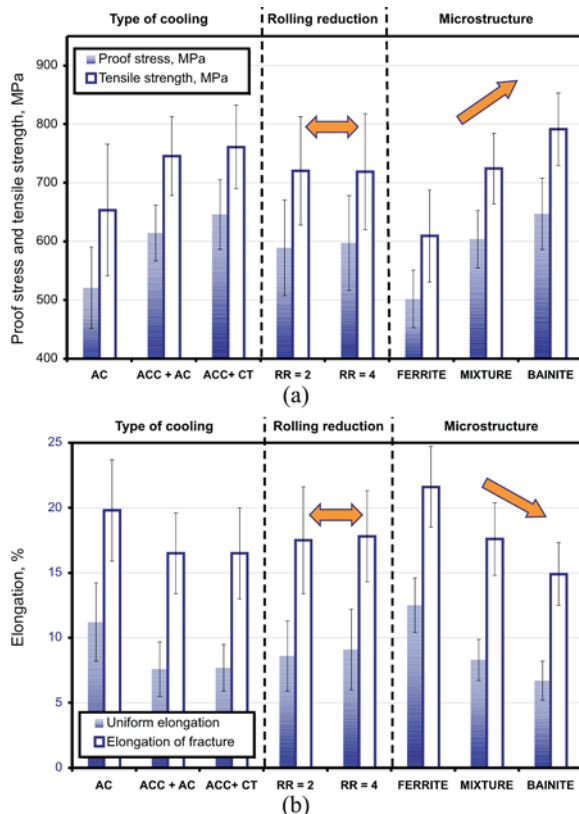


Figure 5 Effects of type of microstructure and rolling conditions on mechanical properties: (a) proof stress and tensile strength, (b) uniform and fracture elongations. Mean values and standard deviations (error bars).

5.3 Multiple regressions

Multiple linear regression technique is used to obtain response equations to response variables: proof stress, tensile strength, uniform and fracture elongations. The sample is formed by the 26 designed casts. Those parameters/variables considered in the three intelligent designs were taken into account (Mn, Ni, Mo, Cr, Cu, C, Nb, B and Ti) for the regression. Also, the rolling parameters, RR , $\lg CR_1$ and $\lg CR_2$ and the interaction terms; $\lg CR_1 \times$ composition terms, $RR \times \lg CR_1$, $Nb \times \lg CR_2$, $RR \times Nb$, $C \times Nb$ and $Ti \times B$, have been included as regressors.

From each parameter, two equations are fitted, showing the results in : These two equations correspond to "Autofit" (first equation) and " R^2_{adj} max" (second equation) methods, where those coefficients with significance $\alpha < 0,1$ (credible ones, statistically proved effects) are shown in bold. From each response method, 3 statistical parameters are shown; coefficient of determination (R^2), adjusted determination coefficient (R^2_{adj}) and the maximum significance (α) which

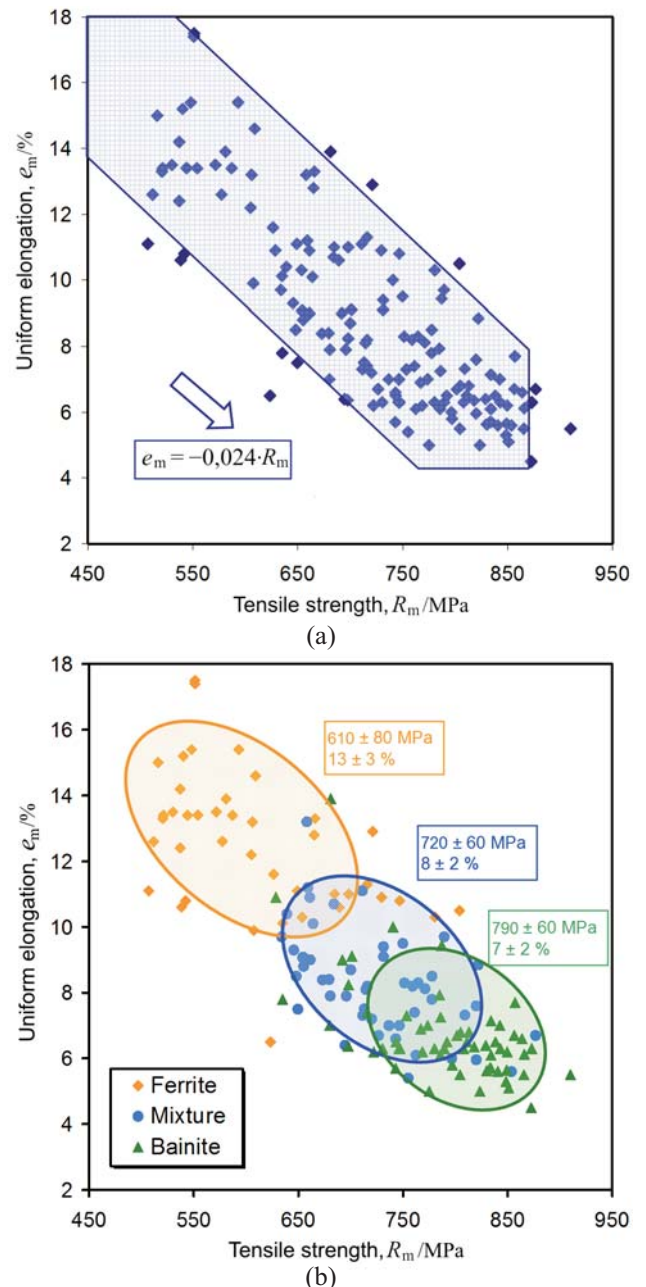


Figure 6 (a) Tensile strength and uniform elongation combinations in low-carbon microalloyed steels with high niobium contents. (b) Effects of type of microstructure on tensile strength and uniform elongation.

present the less credible of the predictor variables (underlined).

From strength models, see Tab. 5a, it is remarkable that tensile strength models obtain better determination coefficients than those for proof stress; 0,888 vs. 0,768 and 0,876 vs. 0,754 for R^2 and R^2_{adj} , respectively (Autofit). This can be explained in terms of discontinuous yielding behaviour (Lüders bands) which the plates often exhibit, making proof stress far more variable than tensile strength. Concerning elongation models, both show similar determination coefficients: 0,713 vs. 0,730 (R^2) and 0,701 vs. 0,714 (R^2_{adj}), for uniform and fracture elongation, respectively.

Again in the case of strength models, see (a), the first terms (single composition terms) predict the strength for $CR = 1$ °C/s ($\log_{10} 1$ °C/s = 0), which is close to air cooling conditions (0,5 °C/s). Conversely, the interaction terms (in brackets) show the correction that needs to be applied for

Table 5 Response equations of tensile test models: (a) strength and (b) elongation

Tensile Tests Models: Strength Models (MPa, wt.%, log(°C/s))	R ²	R ² _{adj}	$\underline{\sigma}_{max}$
Proof Stress (MPa) = 280+61500B+2300Ti+500C+140Mo+70Mn+logCR ₁ (90-23500B)-220Nb×logCR ₂ = 240+61500B+2100Ti+500C+140Mo+90Mn+logCR ₁ (160-24000B-40Mn)-220Nb×logCR ₂ +50RR×Nb	0.768 0.777	0.754 0.761	0.015 0.090
Tensile Strength (MPa) = -45+78000B+4200C +1350Nb+200Mo+190Mn+80Cr+75Ni +logCR ₁ (300-40000B-1000C-70Mn-40Ni)-100Nb×logCR ₂ -19000C×Nb = -40+78000B+4000C+1300Ti+1200Nb+200Mo+180Mn+95Cr+75Ni +logCR ₁ (300-40000B -900C-70Mn-40Ni-40Cu)-100Nb×logCR ₂ -18000C×Nb	0.888 0.891	0.876 0.878	0.083 0.152

Tensile Tests Models: Elongation Models (% , wt.%, log(°C/s))	R ²	R ² _{adj}	$\underline{\sigma}_{max}$
Uniform Elongation (%) = 22-1300B-5Mn-4Mo-2Cr-1Ni-2.7logCR ₁ = 22-1300B-5Mn-4Mo-2Cr-1Ni-2.7logCR ₁ +0.2RR	0.713 0.718	0.701 0.703	0.092 0.148
Elongation of Fracture (%) = 40-2000B-70C-8Mn-6Mo-3Cr-2Ni -2.5logCR ₁ +300C×Nb = 40-2000B-70C-8Mn-6Mo-3Cr-2Ni-1Cu-2.5logCR ₁ +300C×Nb	0.730 0.734	0.714 0.716	0.049 0.166

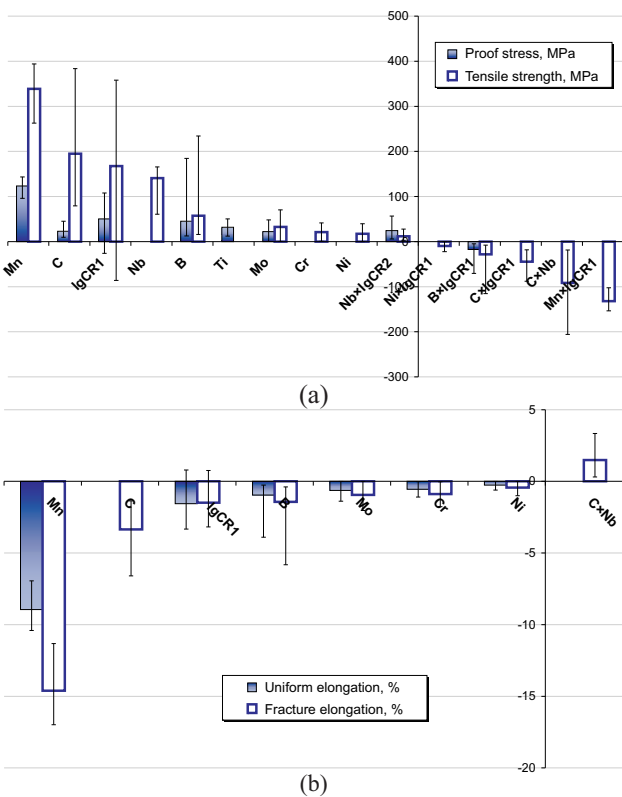


Figure 7 Effects of predictor variables (a) on strength (MPa) and (b) on elongation (%). Average +/- max, minimum effects of significant predictors (Autofit, $\alpha < 0,1$).

faster cooling rates (CR_1 , ACC). As the cooling rate increases, the $\log CR_1$ increases proportionally weakening the effect of such elements ($\log CR_1 \times$ composition terms). On the other hand, Fig. 7a depicts the effect of the proved predictor variables, where the columns represent the average effect and the error bar spans from the maximum to the minimum effect.

From Tab. 5a and Fig. 7a, it is worth to figure out that B, C, Mo, Mn, $\log CR_1$, $Nb \times \log CR_2$ and $B \times \log CR_1$ present significant effects ($\alpha < 0,1$) in both models (proof stress and tensile strength). Concerning significative effects, what is remarkable is the number of interactions terms which appear only in the tensile strength model; $\log CR_1 \times$ composition terms (C, Mn and Ni) and $C \times Nb$, in contrast with proof stress models. The tensile strength values are probably less variable than the proof stress ones,

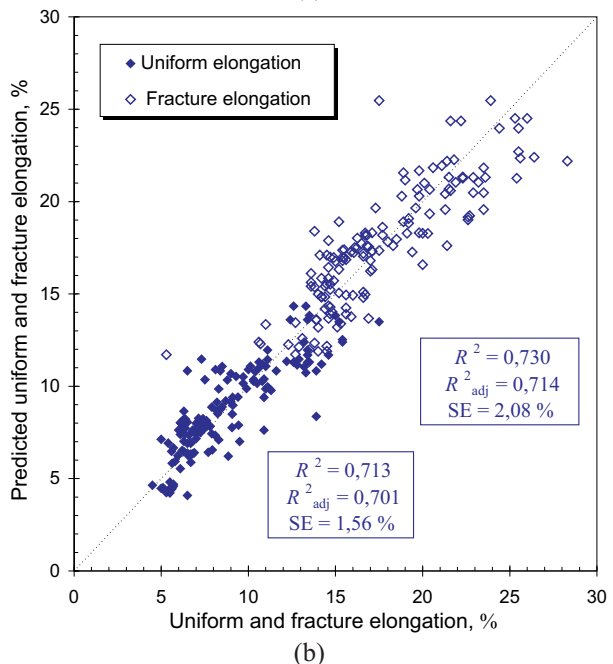
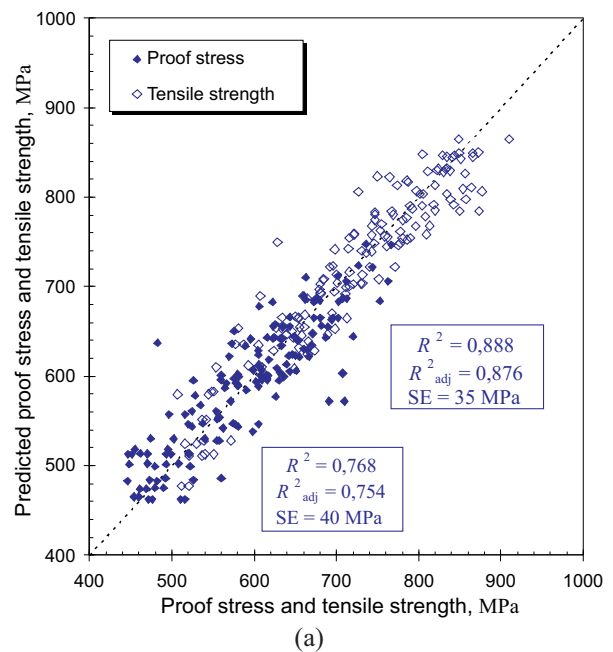


Figure 8 Experimental vs. predicted plots (autofit, model adequacy) for (a) strength, and (b) elongation models

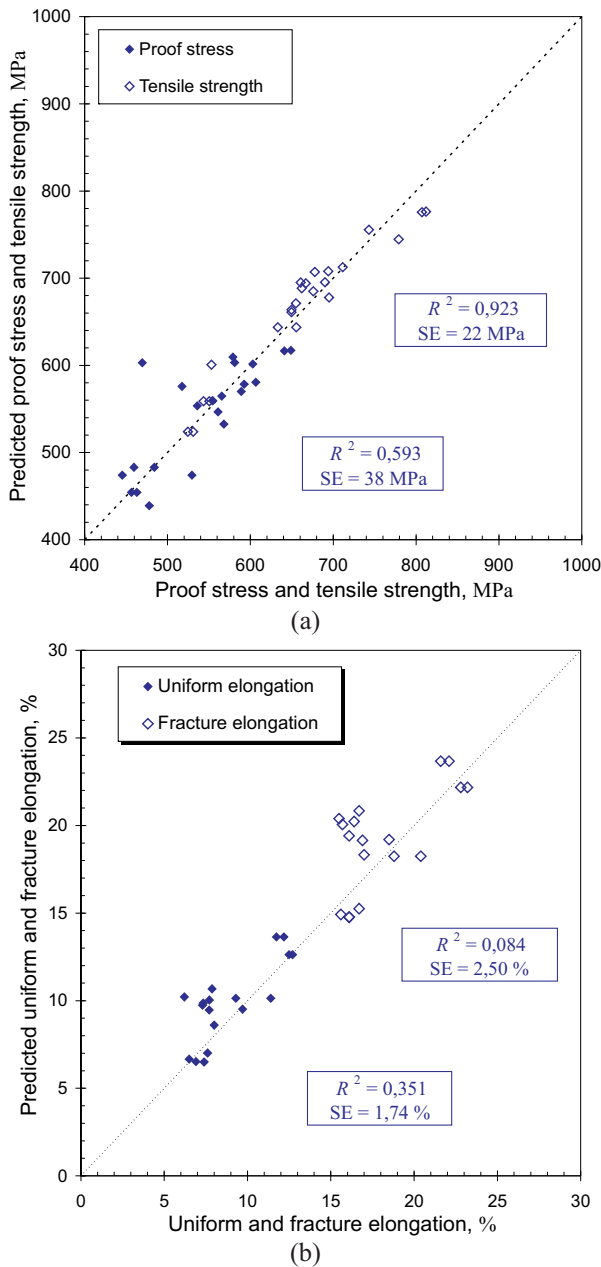


Figure 9 Experimental vs. predicted plots (autofit, model validation) for (a) strength, and (b) elongation models

allowing therefore to obtain a more accurate model (higher coefficient of determinations) and detecting the effects of those regressors which play a minor role (less significant). From elongation models, see Tab. 5b and Fig. 7b, only the interaction term $C \times Nb$ is found to have a significant effect on tensile fracture elongation. Concerning significant effects, B, Mn, Mo, Cr, Ni and accelerated cooling ($\lg CR_1$) present significant effect for both models (uniform and fracture elongations).

Plots of experimental versus predicted parameters were generated for the 26 casts used to compute the response equations, considering only the Autofit method ($\alpha < 0,1$), as shown in Fig. 8. Additional plots, see Fig. 9, show the experimental versus the predicted values for the 4 industrial casts (Tab. 3) to validate the proposed equations (Tab. 5).

If the prediction ability of the proposed equations is checked versus the industrial casts, it is observed that the models predict fairly accurately. The validations show a remarkable determination coefficients of 0,923 for tensile strength, whilst that for the coefficient of proof stress decreases slightly: from 0,768 to 0,593 for model adequacy

(Fig. 8a) and model validation (Fig. 9a), respectively. However, the standard error (SE), which gives an idea of prediction accuracy, is slightly improved; from 40 to 38 MPa.

In the case of elongation models, similar conclusions can be stated when comparing model adequacy with model validation.

5.4 Interactions among response variables

In order to study more deeply the interactions observed chiefly between carbon and niobium on tensile strength, it is interesting to rewrite the response equations plotted in Tab. 5a.

Tensile strength (R_m) =

$$\begin{aligned}
 & -45 + 78000B - 200C + 200Mo + 190Mn + 80Cr + \\
 & + 75Ni + \lg CR_1(300 - 40000B - 70Mn - 40Ni) + \quad (1) \\
 & + C \times [4200 - 19000Nb - 1000 \lg CR_1] + \\
 & + Nb \times [1350 - 19000C - 100 \lg CR_2], \text{ MPa}
 \end{aligned}$$

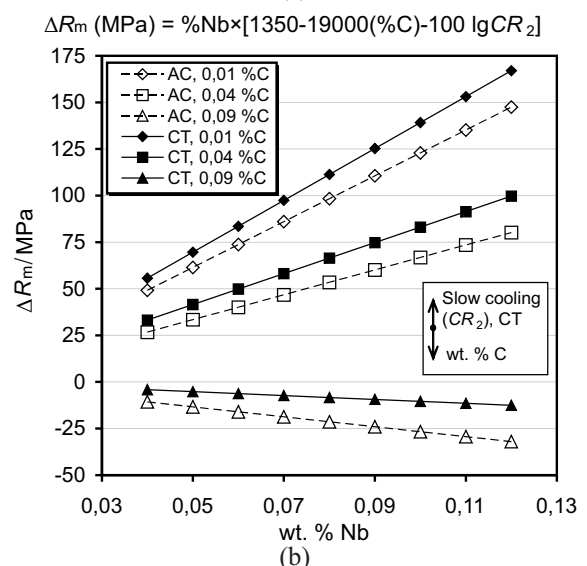
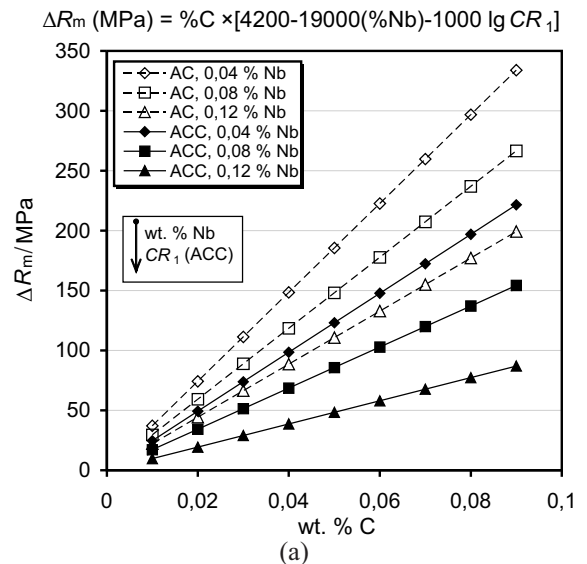


Figure 10 Effect of carbon (a) and niobium (b) on tensile strength

where the alloying elements are introduced as weight percentage (wt. %) and cooling rate (CR_1 , CR_2) as degree per second ($^{\circ}C/s$).

In the equation, which represents the Autofit equation of tensile strength, the terms in which the C and Nb are involved have been rearranged. The above equation tells that additions of B, C, Mo, Mn, Cr, Ni together with accelerated cooling increase the strength level. Conversely, the effect of B, Mn and Ni is weakened as CR_1 is increased, or better said, when accelerated cooling is applied.

Concerning carbon term: $C \times [4170 - 18700Nb - 96 \lg CR_1]$, Fig. 10a has been drawn considering two cooling conditions; AC and ACC, and for three levels of Nb; 0,04, 0,08 and 0,12 %. This latter plot indicates that the carbon effect is weakened when accelerated cooling is applied and for high niobium contents. It seems that carbon is more effective increasing the strength levels for air cooling conditions and in combination with low niobium levels.

In the case of Nb: $Nb \times [1350 - 18700C - 110 \lg CR_2]$, see Fig. 10b, similarly to carbon, it is found that additions of Nb in the range 0,04 and 0,12 % are more effective increasing strength with low carbon contents. Even the model predicts negative effects of niobium when it is accompanied with a carbon content of 0,09 %. On the other hand, the effect of niobium is increased by reducing CR_2 (CT, coiling simulation).

As with tensile strength, the response equation of fracture elongation, Tab. 5b, can be rewritten arranging the carbon terms as follows:

$$\text{Fracture elongation } (e_m) = 40 - 2000B - 8Mn - 6Mo - 3Cr - 2Ni - 2,5 \lg CR_1 - C \times [70 - 300Nb], \% \quad (2)$$

where the chemical composition is introduced as weight percentage (wt. %) and cooling rate (CR_1) as degree per second ($^{\circ}C/s$).

The interaction between carbon and niobium has been plotted in Fig. 11. The results indicate the detrimental effect of carbon on fracture elongation is reduced as the niobium level is increased.

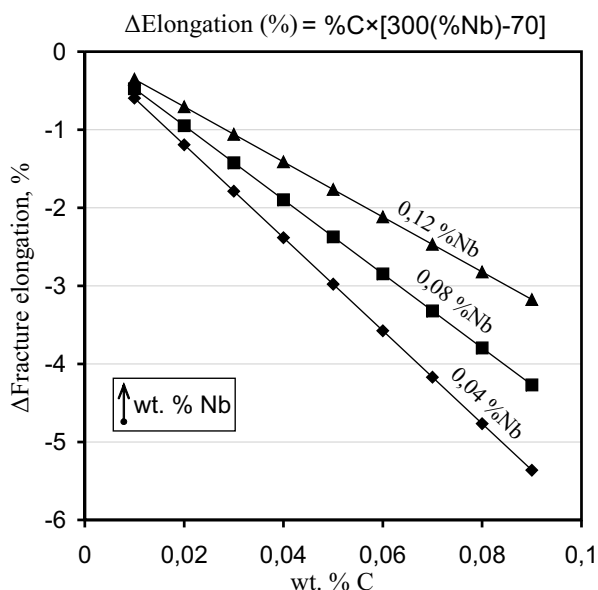


Figure 11 Effect of carbon and niobium on fracture elongation

6 Discussion

In the present work, it was found that high additions of Nb, in the range 0,04 and 0,12 %, are more effective at increasing strength when combined with low carbon contents and with slow cooling rates (coiling). This finding is supported by literature:

It is well known that low carbon contents and fixing of nitrogen with titanium (an element with higher affinity for nitrogen than niobium) prevent niobium carbonitride formation and allow higher niobium contents to be easily dissolved during reheating of the slab, and therefore remaining in solid solution at the commencement of rolling. Besides, low carbon contents provide better toughness and ductility. By further lowering carbon content below the threshold value of 0,09 % (avoiding the peritectic reaction), segregation is reduced [7].

Niobium in solid solution, not precipitated in austenite at the finish rolling temperature, increases the strength by both causing the γ/α transformation to occur at a lower temperature, which results in a higher volume fraction of bainite, and by the formation of niobium carbide precipitates in ferrite by means of slow cooling rates (precipitation hardening). According to equilibrium considerations, the percentage of solute niobium is higher the closer the chemical composition of the steel is to the stoichiometric ratio of carbon to niobium [8]. Thus the amount of solute niobium available for transformation and precipitation becomes greater with reduced carbon in High Strength Low Alloy steels (HSLA) [7, 9].

In hot direct rolling of microalloyed steels with niobium, J. S. Park et al. [10] reported a loss of yield and tensile strength occurred when carbon content exceeded approximately 0,07 wt. %. When carbon content exceeded a critical level, segregation of niobium to the liquid phase during solidification of the castings resulted in the presence of the eutectic NbCN. This effectively removed a significant fraction of the niobium from being able to participate in precipitation strengthening.

On the other hand, the probability of forming niobium carbide precipitates in ferrite or in the austenite-ferrite interphase during phase transformation is well known to be dependent on the finish rolling and cooling conditions. Investigations applying industrial processing cooling rates of more than $10^{\circ}C/s$ from the finish rolling temperature to typical coiling temperatures in the range between 550 and $650^{\circ}C$ did not show ferrite precipitation when typical coil cooling rates of $0,5^{\circ}C/s$ or higher are used [11, 12, 13]. Conversely, K. Hulka [7] found for low carbon microalloyed steels with niobium levels around 0,10 %, that when after transformation at a temperature of $550^{\circ}C$ (the same selected temperature in the present work), slow cooling is applied, ferrite precipitates are promoted giving an additional strength increase by precipitation hardening. Under practical conditions this strength increase was about 40 to 50 MPa. This figure is exactly the same as that obtained in the present work for proof stress; see Fig. 7a, where the upper error bar of $Nb \times \lg CR_2$, which means the effect of slow cooling with high niobium contents, is rather close to 50 MPa.

Concerning elongation, the detrimental effect of carbon on fracture elongation is reduced as the niobium level increases (Fig. 11). Note that the change in strength adversely affects elongation properties (Fig. 6a), therefore the loss of strengthening of carbon, when adding high

niobium contents, is translated into an improvement on elongation properties.

As previously introduced in Fig. 5, the increase of rolling reduction, closely related with grain size refinement [14, 15, 16], surprisingly does not produce an increase in strength as it would be expected (Hall-Petch effect). Note that the rolling reduction (RR) was not found to be significant enough ($\alpha > 0,1$) in tensile test models, see Tab. 5. The explanation of this striking observation can be as follows: The present work deals not only with a unique type of microstructure but with several ones; ferrite, bainite and mixture, being the strength of the latter ones strongly dependent on the transformation temperature [17], giving place to remarkable differences, mainly, in dislocation density and therefore, in strength for a given grain size.

7

Conclusion

- The type of microstructure plays a very important role on mechanical properties, where mean proof stress values of 500, 600 and 650 MPa were observed for ferrite, mixture (ferrite plus bainite) and bainite, respectively.
- The lack of importance of rolling reduction, or Hall-Petch effect on strength may be explained due to the presence of several types of microstructures (ferrite, bainite and mixture), where the type of microstructure plays a far more important role on strength than grain size.
- High Nb contents (up to 0,12 wt. %) are more effective at increasing strength combined with low carbon contents and with slow cooling rates below 550 °C, enhancing precipitation hardening, this latter effect being highly dependent on niobium content.

Acknowledgements

This work has been possible thanks to the ECSC European project (HIPERC) with contract number: RFSR-CT-2005-0007. One of the authors (M. Perez) also wants to thank to FEUN (Fundación Empresa Universidad de Navarra) and to the Torres Quevedo Program of the Spanish Ministry of Education and Science for his fellowship.

8

References

- [1] Pickering, F. B. Towards Improved Toughness and Ductility, Climax Molybdenum, Co. Symp., Kyoto, 1971, p. 9.
- [2] Cuddy, L. J. Metall. Trans., 15^a, 1984, p. 87.
- [3] Thomas, M. H.; Michal, G. M. in H. I. Aaronson et al. (eds.), Solid-Solid Phase Transformation, TMS-AIME, Warrendale, P. A., 1981, pp. 469-473.
- [4] Majta, J.; Kuziak, R.; Pretzyk, M. Journal of Materials Processing Technology, Vol. 80-81 (1998), pp. 524-530.
- [5] HIPERC Project, Final Report (RFSR-CT-20058-00027), pp 51-52.
- [6] Pérez-Bahillo, M.; López, B.; Martín-Meizoso, A. Effect of processing conditions and chemical composition on grain sizes for low-carbon microalloyed steels with high niobium contents, paper in progress.
- [7] Hulka, K. The role of Niobium in Low Carbon Bainitic HSLA Steel, <http://www.msm.cam.ac.uk/phases-rans/2005/LINK/10.pdf>.
- [8] Hulka, K.; Gray, J. M.; Heisterkamp, F.. High Temperature Thermomechanical Processing of Pipe-Steel, Proceeding Pipeline Technology, Ed. by R. Deys, Elsevier (2000), pp. 291-306.

- [9] Klinkenberg, C.; Hulka, K.; Bleck, W. Niobium Carbide Precipitation in Microalloyed Steel, Steel Research int., 75, 11(2004), p. 744.
- [10] Park, J. S.; Ajmal, M.; Priestner, R. ISIJ International, 40, 4(2000), pp. 380-385.
- [11] Itman, A.; Cardoso, K. R.; Kestenbach, H. J. Mater. Sci. and Techn., 13, 1(1997), pp. 49-56.
- [12] Thillou, V.; Hua, M.; Garcia, C. I.; Perdrix, C.; DeArdo, A. J. Proceedings 41st MWSP Conference, ISS, Vol. XXXVII, (1999), p. 471.
- [13] Campos, S. S.; Morales, E. V.; Kestenbach, H. J. Proc. Thermec 2003, Mater. Sci. Forum, 426-432 (2003), pp. 1245.
- [14] Bengochea, R.; López, B.; Gutierrez, I. Metall Trans., 29A, (1988), p. 417.
- [15] Bengochea, R.; Lopez, B.; Gutierrez, I. Proc. of Int. Conf. Microalloying in Steels, Edited by J. M. Rodríguez-Ibabe, I. Gutierrez and B. López, San Sebastian, Spain, (1988), p. 201.
- [16] Tanaka, T. Proc. of Int. Conf. Microalloying 95, ed. by M. Korchynsky, A. J. DeArdo, P. Repas and G. Tither, Pittsburg, USA, (1995), p. 165.
- [17] Irvine, K. J.; Pickering, F. B. J. Iron and Steel Inst., 194, (1960), p. 133.
- [18] ARAMIS, 3D optical extensometers GOM b.H. Braunschweig, www.gom.com

Authors' addresses:

Marcos Pérez-Bahillo

Materials Department, CEIT and Tecnun
University of Navarra
Paseo Manuel Lardizabal, 15
20018, San Sebastian, Spain
E-mail: ameizoso@ceit.es

Nenad Gubelj

Faculty of Mechanical Engineering
University of Maribor,
Smetanova 17, Maribor, Slovenia

David A. Porter

Rautaruukki Oyj, Research Centre,
P. O. Box 93, Raahе, Finland

Beatriz López

Materials Department, CEIT and Tecnun
University of Navarra
Paseo Manuel Lardizabal, 15
20018, San Sebastian, Spain

Jožef Predan

Faculty of Mechanical Engineering
University of Maribor,
Smetanova 17, Maribor, Slovenia

Antonio Martín-Meizoso

Materials Department, CEIT and Tecnun
University of Navarra
Paseo Manuel Lardizabal, 15
20018, San Sebastian, Spain